RESEARCH ARTICLE | AUGUST 08 1997

# Delay-induced chaos in catalytic surface reactions

N. Khrustova; A. S. Mikhailov; R. Imbihl



*J. Chem. Phys.* 107, 2096–2107 (1997)
https://doi.org/10.1063/1.474560

# Delay-induced chaos in catalytic surface reactions

N. Khrustova[a] and A. S. Mikhailov
*Fritz-Haber-Institut der Max-Planck-Gesellschaft, Faradayweg 4-6, 14195 Berlin (Dahlem), Germany*

R. Imbihl
*Institut für Physikalische Chemie und Elektrochemie, Universität Hannover, Callinstr. 3-3a, 30167 Hannover, Germany*

(Received 24 March 1997; accepted 28 April 1997)

Deterministic chaos related to a sequence of period-doubling bifurcations (the Feigenbaum transition) has been observed in the NO+CO and NO+$H_2$ reactions on Pt(100). On a microscopic scale, these reactions are accompanied by the formation of 1×1 adsorbate islands due to the properties of the 1×1↔hex phase transition of Pt(100). A simple skeleton model is constructed that describes the behavior of a population of reacting islands which are globally coupled together via the gas phase. Investigations of this model show that the experimentally observed chaotic behavior can result from delays in the response of the reacting islands to partial pressure variations in the gas phase. © *1997 American Institute of Physics.* [S0021-9606(97)00330-9]

## I. INTRODUCTION

Complex aperiodic behavior of catalytic surface reactions has been observed under various conditions ranging from high-pressure experiments ($p>1$ mbar) with supported catalysts to low-pressure single crystal studies ($p<10^{-3}$ mbar) conducted under isothermal conditions.[1,2] For some of these experiments detailed analyses have been conducted demonstrating that the aperiodic oscillations were not caused by experimental irregularities but represent deterministic chaos. The interpretation of the high-pressure experiments is complicated due to the nonisothermality of the reaction and due to the nonuniformity of the catalysts. Conceptually simpler are single-crystal experiments where deterministic chaos has been identified in three systems; Pt(110)/CO+$O_2$,[3] Pt(100)/NO+$H_2$,[4] and Pt(100)/NO+CO.[5] In all three systems a transition from regular oscillations to chaos took place via a sequence of period-doublings (the Feigenbaum scenario).

For each of these systems mathematical models are available which reproduce well the stationary and oscillatory behavior of the reactions.[6–10] It is therefore quite a surprise that so far all attempts to simulate the experimentally observed chaotic oscillations by modifying the existing sets of differential equations were fruitless. A conclusion which could be drawn from these negative results is that perhaps not the properties of an individual oscillator are responsible for the occurrence of chaos, but that it is rather the interaction between different local oscillators which is causing chaos.

The purpose of this paper is to demonstrate that the synchronization of a whole population of individual oscillators which are tied together via global coupling can in fact give rise to deterministic chaos. We show this by setting up a skeleton model for two experimentally investigated systems, Pt(100)/NO+CO and Pt(100)/NO+ $H_2$.[11] In the model we only incorporate those mechanistic steps which we believe are essential for the occurrence of chaotic behavior. The analysis of this simple model of a hypothetical monomolecular chemical reaction shows that delays in the response of reactive islands to partial pressure variations in the gas phase can indeed lead to the onset of chaotic oscillations in the global reaction rate. In addition, it is shown that the bifurcation diagram of this model agrees qualitatively with the sequence of instabilities observed in the experiment. Furthermore, we consider possible modifications of the basic model and analyze how the transition to chaos and the properties of chaotic oscillations are influenced by incorporation of additional mechanistic details of the reaction.

## II. CHAOTIC BEHAVIOR IN THE NO+CO REACTION ON Pt(100)

A serious difficulty faced in the analysis of chaotic data from surface reactions is that the role which the spatial degrees of freedom play in the development of chaotic behavior is usually unknown. To avoid this problem, we choose a system which has been shown to react spatially uniformly during the chaotic rate oscillations. This is the case for the rate oscillations which occur in the NO+CO reaction on a largely hex reconstructed Pt(100) surface, as demonstrated by spatially resolved *in situ* measurements with photoemission electron microscopy (PEEM).[5]

The clean Pt(100) surface in its thermodynamically stable state exhibits a quasihexagonal reconstruction of the top layer of metal atoms (''hex'').[12] The reconstruction can reversibly be lifted by adsorption of glasses like CO, NO, $H_2$, etc. This constitutes an adsorbate-induced surface phase transition between the bulklike 1×1 and the reconstructed hex phase, 1×1↔hex, which is controlled by critical adsorbate coverages.[12–21] The properties of the CO-induced surface phase transition have been extensively investigated with a number of techniques like low energy electron diffraction (LEED),[12,15] vibrational spectroscopy,[12,14,19] scanning tunneling microscopy (STM),[13,18] molecular beam

[a]On leave from N. N. Semenov Institute for Chemical Physics, Russian Academy of Sciences, ul. Kosygina 4, 117333 Moscow, Russia.

 0021-9606/97/107(6)/2096/12/$10.00 

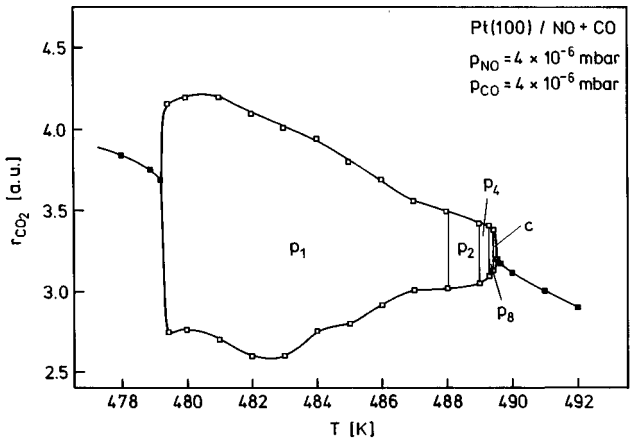


FIG. 1. Experimental bifurcation diagram for the rate oscillations in the NO+CO reaction on Pt(100)-hex (Ref. 4). Filled squares mark a stationary $CO_2$ production rate, $r_{CO_2}$, while the open squares mark the upper and lower turning points of the rate oscillations. $P_1$, $P_2$, $P_4$, and $P_8$ represent the periodicities which were identified in the experiment; $C$ marks the region where chaotic oscillations were found.

experiments,[16,17] and microcalorimetry.[20] The driving force for the lifting of the hex reconstruction by CO has been shown to lie in the gain in adsorption energy which is about 28 kJ/mol higher on the 1×1 phase than on the hex phase ($\theta_{CO}=0.5$).[12,20]

Kinetic oscillations in the NO+CO and in the NO+$H_2$ reaction both occur under very similar conditions, i.e., in the vicinity of the phase transition as the hex-reconstructed surface is cooled down in a NO/CO (NO/$H_2$) atmosphere. On the cooling branch the oscillations develop in a narrow temperature interval where the adsorbate coverage just becomes high enough to initiate the lifting of the hex reconstruction by the growth of mixed 1×1-CO,NO islands.[5,7] The oscillations take place on a largely hex-reconstructed surface and they are coupled to the 1×1↔hex phase transition. The phase transition modulates the catalytic activity because only the 1×1 phase can dissociate NO and therefore is catalytically active while the hex phase is ineffective in that respect.[7] As shown by the bifurcation diagram in Fig. 1, coming from high temperature first small amplitude chaotic oscillations develop which then with decreasing temperature grow in amplitude while undergoing a Feigenbaum cascade in reverse direction.[5]

In order to create a homogeneously oscillating surface, an efficient coupling mechanism has to exist which can synchronize the local oscillators. This coupling mechanism is provided by the small partial pressure variations of the reactants (on the order of a few percent) which accompany the rate oscillations and which arise due to mass balance in the reaction. Since the reaction chamber under low-pressure conditions ($p<10^{-3}$ mbar) can be described as a gradient-free flow reactor, these variations represent global coupling. Under oscillatory conditions the adsorbate coverage on the hex phase is near the critical coverage for the phase transition and therefore small variations in $p_{NO}$ or $p_{CO}$ can very efficiently synchronize the reacting surface via the phase transition.

The spatial homogeneity of the oscillating surface which is seen in PEEM exists, however, only on a macroscopic scale (>1 $\mu$m), while on a microscopic scale the different surface phases form islands. Mainly due to a larger adsorption energy the adsorbing CO,NO-molecules are forced into 1×1 islands with a high local coverage of about 0.5, while the surrounding hex area remains largely adsorbate-free.[12,13,18] From the results of adsorption studies of Pt(100)/CO with STM, LEED, and vibrational spectroscopy one can estimate their size to lie in the range between 10 and 1000 Å.[12–14,19] Since NO and CO behave very similar with respect to the phase transition and since no strong attractive or repulsive interactions exist between CO and NO molecules on the 1×1 phase we assume that they form mixed 1×1-CO, NO islands.[19]

The reaction of the molecular adsorbates to the products $N_2$ and $CO_2$ according to $CO_{ad}+NO_{ad}\rightarrow CO_2+1/2N_2$ proceeds via the dissociation of NO. Due to the vacant site requirement for NO dissociation the reaction between the molecular adsorbate takes place in a step

$$NO_{ad}+CO_{ad}+*\rightarrow 1/2N_2+CO_2+3*$$

in which the number of vacant adsorption sites (*) increases autocatalytically. This autocatalytic reaction is responsible for the occurrence of a so-called ''surface explosion,'' i.e., a rapid reaction between the two adsorbates which takes place when the combined CO/NO coverage falls below the inhibition coverage for NO dissociation of 0.5.[22,23]

Under oscillatory conditions the 1×1 islands naturally have to grow and dissolve again and one can construct the following life cycle. Starting with the unreactive hex phase CO and NO will adsorb on the hex phase and initiate the nucleation of mixed 1×1-CO,NO islands. As these islands trap diffusing NO, CO molecules from the surrounding hex phase, they grow while maintaining a constant local coverage of ≈0.5. The islands grow as unreactive molecular adsorbate islands but since the growth coverage of 0.5 is identical with the inhibition coverage for NO dissociation, the stability of these islands lies on a critical borderline. Therefore the islands remain unreactive only until they reach a critical radius above which the ''surface explosion'' sets in, leading to the rapid reactive removal of the molecular adsorbate. The reactive islands accordingly have a low adsorbate coverage. The low coverage 1×1 areas, being no longer stabilized by the adsorbate, relax back into the hex phase. This relaxation process is strongly activated.[12,15,20]

It is evident that without synchronization the contribution of the independently oscillating islands would add up to a constant average value. Synchronization in the NO+CO and NO+$H_2$ reactions on Pt(100) has been attributed to the 1×1↔hex phase transition and recent findings helped to formulate a precise physical law for the dependence of the phase transition on partial pressure variations. Employing molecular beam techniques to the system Pt(100)/CO, it was demonstrated by King *et al.* that the growth rate, $r_{grow}$, of the 1×1 phase during the CO-induced lifting of the hex reconstruction obeys a power law of the form $r_{grow}\sim(\theta_{CO}^{hex})^{4.5}$ in which $\theta_{CO}^{hex}$ denotes the CO coverage on the hex phase.[16,17]

A similar power law has also been determined for the hydrogen-induced lifting of the hex reconstruction on Pt(100).[21]

Homogeneous nucleation was initially suggested but subsequent STM investigations by Borg *et al.* showed that the $1\times1$-CO islands nucleate preferentially at step edges.[18] This latter result indicates heterogeneous nucleation and, in order to make this nucleation mechanism compatible with the power law, one has to assume that either also in the case of heterogeneous nucleation several CO molecules are required to form a critical nucleus or, alternatively, that this number is necessary to allow for the further growth of an already existing nucleus.

In the presence of reactions, heterogeneous nucleation should be stronger since the Pt(100) surface under reaction conditions is no longer an ideal plane surface but will be roughened.[7,24] The main contribution to this roughening can be attributed to the $1\times1\leftrightarrow$hex phase transition since the density of surface atoms is about 20% higher in the hex than in the $1\times1$ phase.[13,18] A mass transport of Pt atoms is thus required and in a reacting environment the dynamics of the reaction in connection with this mass transport cause a substantial roughening of the Pt surface as was demonstrated experimentally.[24] Real space images not of the reaction-induced roughening but of roughening caused by the CO-induced lifting of the hex reconstruction can be found in STM studies of Pt(100)/CO.[13,18]

## III. THE MATHEMATICAL MODEL

Detailed mathematical models of the NO+CO and NO+$H_2$ reactions have been constructed that incorporate the major known reaction steps[7–10] and take into account the experimentally determined power law for the growth of the $1\times1$ phase.[8,10] The analysis of these models, however, reveals that, though they reproduce a transition to oscillations in the reaction system and yield satisfactory estimates for the oscillation period (cf. Refs. 7–10), they suffer from a principal qualitative disagreement with the experiments, since they do not describe a transition from oscillations to chaos characteristically observed in the experiments.[4,5,25]

The transition to chaos and even the sequence of instabilities leading to such a transition are apparently similar for several chemical reactions whose detailed mechanisms must be significantly different (see the discussion above). This suggests that the effect responsible for this transition is not just a minor detail of a particular reaction mechanism. Rather, it should be a generic property of a certain class of surface chemical reactions.

A general property underlying destabilization of regular oscillations and leading to the development of chaos in dynamical systems is often a time delay in the feedback loops leading to persistent self-oscillations. This mechanism is responsible for chaotic oscillations in such different systems as, for example, ecological populations,[26] the physiological respiration system,[27] or nonlinear optical systems.[28,29]

Therefore one can ask whether a similar delay mechanism may be operating in systems with surface chemical reactions when a transition to chaos is observed. Looking again at these reactions, we see that there should be a period between the nucleation of an adsorbate island and the moment when a chemical ''explosion'' takes place, leading to the destruction of this island. When the existence of this period is taken into account, a delay is effectively added to the feedback loop responsible for oscillations in the system. Indeed, the nucleation rate of islands is controlled by the partial pressure of the adsorbate in the gas phase which, in turn, is influenced by the current reaction rate. The essential point, however, is that the islands contribute to the global reaction rate only after a certain time has passed after their nucleation, i.e., when they become reactive through ignition of the ''surface explosion'' inside the islands.

As a simple skeleton model which takes into account only the essential aspects of the considered reactions, we consider a hypothetical monomolecular reaction $X\rightarrow Y$ taking place on the surface of a catalyst inside a gas flow reactor. In the following we describe a general model but the transition to the surface reaction on Pt(100) can easily be made by replacing ''unreactive area'' by ''hex phase,'' ''unreactive islands'' by ''$1\times1$-CO,NO islands'' and ''reactive area'' by ''low coverage $1\times1$ surface.''

The reaction $X\rightarrow Y$ proceeds only on small reactive islands, while the surrounding surface area has no catalytic activity. The product molecules $Y$ do not participate further in the reaction. The reactive islands can be viewed as a population of microreactors randomly scattered over the surface. Such microreactors are, however, not static; each of them is spontaneously created, passes a certain dynamical cycle, and then dies out.

The life-cycle of an individual island is described by the following sequence. The island is nucleated and begins to grow. When a certain critical age is reached, it becomes reactive, i.e., it is transformed into a local chemical microreactor where the conversion reaction $X\rightarrow Y$ goes on. The molecules $X$ participating in this reaction arrive from the gas phase. The reactive stage of an island lasts for some time and after that the island dies out.

In our simple model we do not specify the processes responsible for transformation to the reactive state and the final death of an island. Moreover, we assume that the ''ignition'' time $\tau$ is identical for all islands. The death of an island is, however, a statistical event characterized by a certain mean decay rate.

We consider a situation where the fraction of the surface area occupied by both reactive and nonreactive islands is small. Therefore, interactions between the islands can be neglected. Moreover, the diffusion flow of adsorbed molecules $X$ into the islands is relatively small, so that the mean coverage of molecules $X$ outside of the islands is mainly determined by adsorption and desorption processes. This coverage, however, controls the nucleation rate of new islands, thus establishing a nonlinear feedback in the system.

If $p$ is the partial pressure of molecules $X$ in the gas phase, $c$ the mean adsorbate coverage outside of islands, and $q$ the total surface area occupied by reactive islands, this model is described by equations

$$\dot{c} = -\gamma c + \alpha p(1-c), \tag{1}$$

$$\dot{p} = -\Gamma(p-p_0) - kpq, \tag{2}$$

$$\dot{q} = -\mu q + w. \tag{3}$$

According to Eq. (1), the evolution of coverage $c$ in the area outside of the islands is determined by adsorption and desorption of molecules $X$ on the surface ($\alpha$ contains the sticking coefficient of the $X$ molecules and $\gamma$ is the desorption rate constant). Equation (2) is a standard continuous-flow stirred-reactor equation. The pumped gas flow reactor is characterized by a residence time $t_{\mathrm{res}} = 1/\Gamma$, the partial pressure of molecules $X$ in the gas phase in absence of a reaction is $p_0$. The last term in this equation takes into account the consumption of molecules $X$ in the reaction. Since the reaction $X \rightarrow Y$ proceeds when molecules $X$ from the gas phase impinge on the reactive islands, the rate is proportional to the product of the total area $q$ covered by all reactive islands and the partial pressure $p$ of $X$ in the gas phase ($k$ is the reaction rate constant).

Equation (3) describes the evolution of the total reactive area $q$. The first term here takes into account the decrease in the reactive area due to the death of the islands. The second term $w$ represents the production rate of the new reactive area. In the model each island becomes reactive, and thus contributes to the total reactive area only, when it reaches the critical age $\tau$ at which point it has the critical radius $R$. Therefore, we have $w = \pi R^2 s$, where $s$ is the nucleation rate of islands for the entire surface at an earlier time moment $t-\tau$.

STM experiments indicate that heterogeneous nucleation of islands plays a dominant role[18] so that new islands are built around structural defects which are present on the surface. Generally, these structural defects facilitate nucleation, but do not immediately trigger it. In other words, the microscopic nucleation stage would generally involve a stochastic growth of a cluster of adsorbed molecules on a structural defect until this cluster reaches a critical size and further deterministic growth of an island becomes possible. The process of stochastic subcritical growth may be very sensitive to the surface concentration of adsorbed molecules, i.e., on their average $c$. On the other hand, the rate of heterogeneous nucleation should be proportional to the local density of structural defects. Therefore, the nucleation rate is given by

$$s = \kappa n f(c), \tag{4}$$

where $f(c)$ is a nonlinear function of the coverage, $n$ is the number of structural defects, and $\kappa$ is a proportionality factor.

Collapse and destruction of reactive islands, which takes place as a result of the reaction, produce a large number of temporary structural surface defects that can also serve as nucleation centers for the islands. Therefore, the total number of structural defects on the surface is given by a sum $n = n_0 + n_1$ where $n_0$ is the number of permanently present static surface defects and $n_1$ is a time-dependent number of temporary defects created by the reaction.

We assume that the latter defects vanish very rapidly in a thermal reordering process. In a rough approximation, we can set therefore the number $n_1$ of such defects proportional to the total reaction rate. Since, according to Eq. (2), the reaction rate is $r = kpq$, we have $n_1 = \zeta pq$, where $\zeta$ is a proportionality constant. Therefore, the total nucleation rate of islands can be written as

$$s = \kappa(n_0 + \zeta pq) f(c), \tag{5}$$

where the first term in the parentheses corresponds to heterogeneous nucleation on static surface defects and the second term takes into account reaction-induced heterogeneous nucleation. It is assumed that both processes are characterized by the same coverage dependence $f(c)$.

Our analysis will demonstrate that heterogeneous nucleation on the defects produced by the reaction plays a central role in the transition to chaotic oscillations. To show this, we first completely neglect heterogeneous nucleation at permanent structural defects which is equivalent to putting $n_0 = 0$ in Eq. (5). We also choose, as a simple approximation, a power-law dependence of the nucleation rate on the adsorbate coverage $c$, i.e., we assume that $f(c) = f_0 c^{\nu}$, where $\nu$ is a numerical constant. Under these approximations, the total growth rate $w(t)$ of new reactive area on the surface at the moment $t$, determined by the islands that have nucleated at an earlier moment $t-\tau$ and reach the reactive stage at this time, is given by the equation

$$w(t) = Ac(t-\tau)^{\nu} p(t-\tau) q(t-\tau). \tag{6}$$

Here the coefficient $A$ combines several proportionality factors.

An important parameter in the presented skeleton model is the heterogeneous nucleation exponent for the $1\times1$ phase $\nu$ in Eq. (6). No direct measurements of this exponent are available. In molecular beam experiments by King *et al.* on the CO-induced lifting of the hex reconstruction on Pt(100) only the growth exponent for the total area of the $1\times1$ phase has been determined.[16,17] This exponent is identical with the nucleation rate exponent only under the condition that the islands after their nucleation grow with a constant rate independent of the coverage on the hex phase. Initially both homogeneous and heterogenous nucleation have been considered as realistic possibilities,[13,16] but subsequent STM measurements of Borg *et al.* gave a clear indication towards heterogeneous nucleation since the STM measurements showed that the CO-islands develop preferentially near step edges.[18]

A suggested explanation of the experimentally found dependence is that several molecules have to come together in order to initiate restructuring of the hex phase in a concerted reaction step.[16,17] This concerted reaction step could be the formation of a critical nucleus at a structural defect in which case the nucleation rate would be rate-limiting for the growth of the $1\times1$ area. Alternatively, several CO molecules would be required to allow for the further growth of an already existing supercritical $1\times1$-CO island. The exponent for the nucleation rate would be unknown then. Since the experi-

mental data did not allow us to discriminate between the two alternatives we chose the first interpretation which physically is more intuitive.

A detailed discussion of the observed dependence[16,17] is not very important to us since the conditions of these experiments were essentially different from the conditions under which the chaotic rate oscillations have been observed. The experiments[16,17] were conducted (i) only for CO and not for NO, (ii) in the absence of a reaction, and (iii) the surface was a well annealed hex phase whereas the NO+CO reaction took place on a hex surface roughened by the reaction. Moreover, the data for the growth exponent were collected only in a temperature range from 380 to 410 K while the chaotic oscillations are observed at a much higher temperature of 480 K.[5]

In the measurements on Pt(100)/CO the exponents $\nu=3.9$, 4.7, 5.4, and 5.8 were obtained for the temperatures $T=380$, 390, 400, and 410 K, respectively, and an average $\nu=4.5\pm0.4$ has thus been deduced.[16,17] A linear extrapolation of these data predicts a growth exponent of about $\nu=9$ at the temperature $T=480$ K.[11] King has pointed out[30] that the experimental error is too large to deduce a temperature dependence of the growth exponent but apparently the published data do also not contradict the assumption of higher growth rate exponents at larger temperatures.

In this paper we refer to the measurements in Refs. 16 and 17 only in the sense that they indicate a strong sensitivity of the island nucleation and growth properties on the adsorbate coverages. Since we cannot estimate the exponent $\nu$ from the experimental data, we allow this parameter to vary in our simulations in order to see how the predicted behavior would depend on its value.

In the next section, we perform a detailed analysis of the dynamical model constituted by differential Eqs. (1)–(3) with the time-delay introduced by Eq. (6).

## IV. TRANSITION TO CHAOS

To analyze the dynamical behavior of the system described by Eqs. (1)–(3) with the time-delayed term (6), we first simplify the model and introduce dimensionless variables.

In the model the coverage $c$ in the area outside of the islands remains small, i.e., $c\ll1$. This means that the desorption rate $\gamma$ is much larger than the desorption rate and hence the coverage $c$ adiabatically adjusts to partial pressure variations. In the adiabatical approximation, Eq. (1) yields

$$c=(\alpha/\gamma)p. \tag{7}$$

Introducing dimensionless variables $x=p/p_0$ and $y=kq/\Gamma$ and measuring time in units of the delay time $\tau$, Eqs. (1)–(3) and (6) are then reduced to a system of two differential equations with a time delay,

$$G^{-1}\dot{x}+x=1-xy, \tag{8}$$

$$g^{-1}\dot{y}+y=a[x(t-1)]^{\nu+1}y(t-1), \tag{9}$$

where the new coefficients are $G=\Gamma t$, $g=\mu\tau$, and $a=A\alpha^{\nu}{p_0}^{\nu+1}/\mu\gamma^{\nu}$.

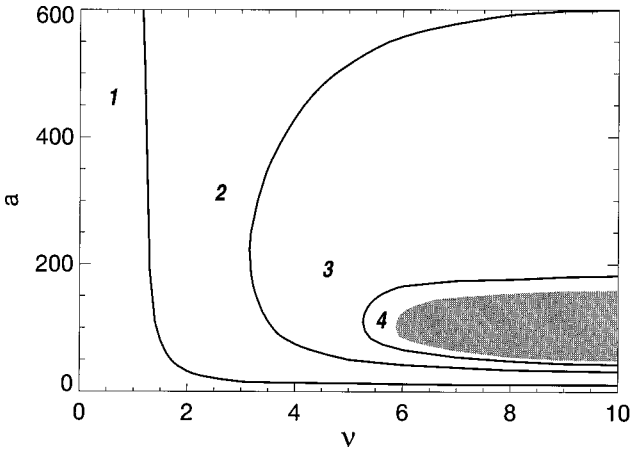


FIG. 2. Bifurcation diagram in the plane $(a,\nu)$ for the dynamical systems (8) and (9) for $G=16$ and $g=8$; (1) damped oscillations resulting in a stable steady state, (2) period-1 oscillations, (3) period-2 oscillations, (4) period-4 oscillations. Long-period and chaotic oscillations are found inside the gray region.

Some insight into the dynamical properties of this model can be obtained by considering a time-delay differential equation, to which systems (8)–(9) reduce in the case when $G\to\infty$,

$$g^{-1}\dot{y}+y=\frac{ay(t-1)}{[1+y(t-1)]^{\nu+1}}. \tag{10}$$

We note that Eq. (10) is similar to the delay equation

$$g^{-1}\dot{y}+y=\frac{ay(t-1)}{1+y^{\nu}(t-1)}, \tag{11}$$

which has been formulated to describe complex physiological oscillations[15] and where period-doubling bifurcations leading to chaos have first been observed for a time-delay differential equation.

Moreover, we can look at the difference equation, to which systems (9) and (10) are reduced in the singular limit $G\to\infty$, $g\to\infty$. This equation, representing the iterative map

$$y(t)=\frac{ay(t-1)}{[1+y(t-1)]^{\nu+1}}, \tag{12}$$

exhibits[14] a transition to chaos through a sequence of period-doubling bifurcations with increasing the bifurcation parameters $a$ or $\nu$ (the chaotic oscillations are then found for $\nu>2$ and $a>14.77$).

Previous analyses of dynamical systems with time delays, describing complex physiological oscillations[28] and effects of optical bistability,[29,30] have shown that the behavior of such systems could be very close to that found in the singular limit for a respective discrete map. A similar behavior can thus be expected for systems (9) and (10).

We have performed a systematic numerical integration of Eqs. (9) and (10). By repeating integrations for various choices of the parameters, we have constructed an approximate bifurcation diagram for the dynamical systems (9) and (10) in the plane $(a,\nu)$ which is displayed in Fig. 2. As

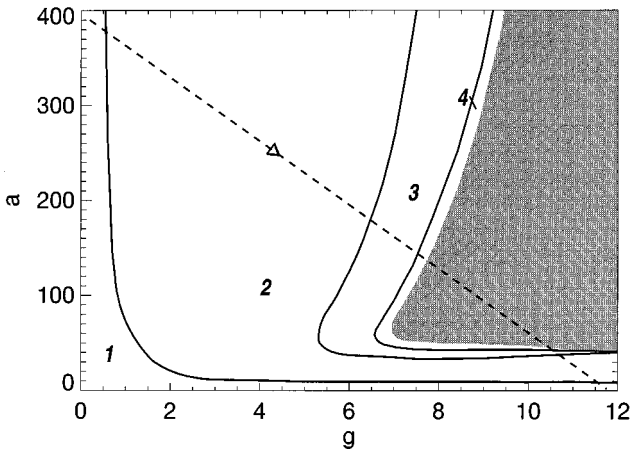


FIG. 3. Bifurcation diagram in the plane $(a,g)$ for the dynamical systems (8) and (9) for $G=16$ and $\nu=9$; (1) stable steady state, (2) period-1 oscillations, (3) period-2 oscillations, (4) period-4 oscillations. Complex oscillations and chaotic regimes are found inside the gray region. The dashed line with the arrow schematically shows how this diagram is traversed with increasing temperature.

already expected from the behavior found in the respective map,[12] chaotic oscillations in the model (9)–(10) exist only for a sufficiently large value of the exponent $\nu$, i.e., for $G=16$ and $g=8$ they are observed only when $\nu>6$. Thus the strong power-law dependence of the nucleation rate $c^{\nu}$ on the coverage $c$ is essential for the existence of a chaotic regime in this model. The transition to chaos takes place through a sequence of period-doubling bifurcations, i.e., according to the Feigenbaum scenario.

Figure 3 shows the typical bifurcation diagram in the plane $(a,g)$ for $\nu=9$. We see that a large part of this plane is occupied by the region 2 where simple limit-cycle oscillations are observed. They originate by a Hopf bifurcation from the stable steady state as the boundary separating regions 1 and 2 is crossed. The upper right part of the diagram is occupied by a region (gray area in Fig. 3) where chaotic oscillations or high-period oscillations (see below) are observed. This region is separated from region 2 by band-shaped regions 3 and 4 where, respectively, oscillations with periods 2 and periods 4 are found.

Though the phenomenological model which we now investigate does not represent a realistic approximation of the actual surface chemical reaction studied in the experiments, it might still be interesting to compare qualitative features of the bifurcation diagram obtained by simulations of this model with the sequence of instabilities found in the experiments by increasing the temperature.

In order to establish a correspondence between Fig. 3 and the experimental sequence in Fig. 1, we note that, when the temperature rises, both the desorption rate $\gamma$ and the decay rate of the reacting islands $\mu$ should increase. Since the parameter $a$ in Eq. (9) is proportional to $\mu^{-1}\gamma^{-\nu}$ with $\nu=9$, $a$ has to decrease rapidly with temperature. On the other hand, the parameter $g$ is proportional to $\mu$ and therefore slowly grows with temperature. Hence, as the temperature is gradually increased, the bifurcation diagram in the plane $(a,g)$ is traversed in the direction schematically indicated by the dashed line in Fig. 3.

We see that at lower temperatures a stable steady state is found. As the temperature increases, small-amplitude limit-cycle kinetic oscillations develop through a Hopf bifurcation. These oscillations remain stable in a relatively wide temperature interval. The amplitude of the oscillations slowly grows with temperature. When a certain critical temperature is reached, the oscillation period is doubled. Through subsequent period doublings chaotic oscillations are finally established in the system.

Such chaotic oscillations are observed inside a relatively large temperature interval, corresponding to the gray region in Fig. 3. Note that not the entire gray region is occupied by the chaotic regime. Actually, inside this region one also finds many narrow windows of periodic oscillations. Since the correct mapping of all these windows requires great computational efforts, we do not show them in Fig. 3, as well as in other bifurcation diagrams in this article.

When the temperature is further increased, a rapid inverse sequence of period-doubling bifurcations is observed. This sequence leads back to the stationary steady state. Examination of Fig. 3 shows that this inverse bifurcation sequence occurs within a very narrow temperature interval. Probably, for this reason this transition has not been resolved in the experiments.

Typical time series of the reaction rate $r$, proportional to the product $xy$, inside different regions in the bifurcation diagram are shown in Fig. 4. We see that the system displays simple limit-cycle oscillations [Fig. 4(a)], stable oscillations with higher periods [Figs. 4(b), 4(c), 4(e), and 4(f)], and complex irregular oscillations [Fig. 4(d)]. The computation of the maximal Lyapunov exponent for the latter complex oscillations shows that the exponent is positive ($\lambda\approx 0.2$), and therefore they can be described as chaotic.

Inside the gray region in Fig. 3, where chaotic oscillations are observed, one finds windows of oscillations with periods 3, 5, 7,... [Fig. 4(e) shows an example of period-3 oscillations]. This is a common feature of different systems with a Feigenbaum scenario.[31] Remarkably, such windows inside the chaotic region have also been observed in the experiments with the $NO+H_2$ reaction on Pt(100)-hex.[4]

Thus, although the model presented here is a skeleton model and neglects all details of the reaction, it qualitatively reproduces the dynamical behavior found in the NO+CO and the $NO+H_2$ reaction on Pt(100)-hex.[4,5]

In the above simulations we neglected heterogeneous nucleation of islands on permanently present defects, i.e., it was assumed that new islands nucleate only at the temporary defects left by the decaying reactive islands. Below we discuss the effects appearing when such heterogeneous nucleation at static defects is taken into account. According to Eq. (5), the inclusion of heterogeneous nucleation of islands on static defects leads to a modification of Eq. (6) for the rate $w$ of appearance of new reactive area on the surface. Now it should have the form

$$w(t)=Ac^{\nu}(t-\tau)p(t-\tau)q(t-\tau)+Bc^{\nu}(t-\tau), \qquad (13)$$

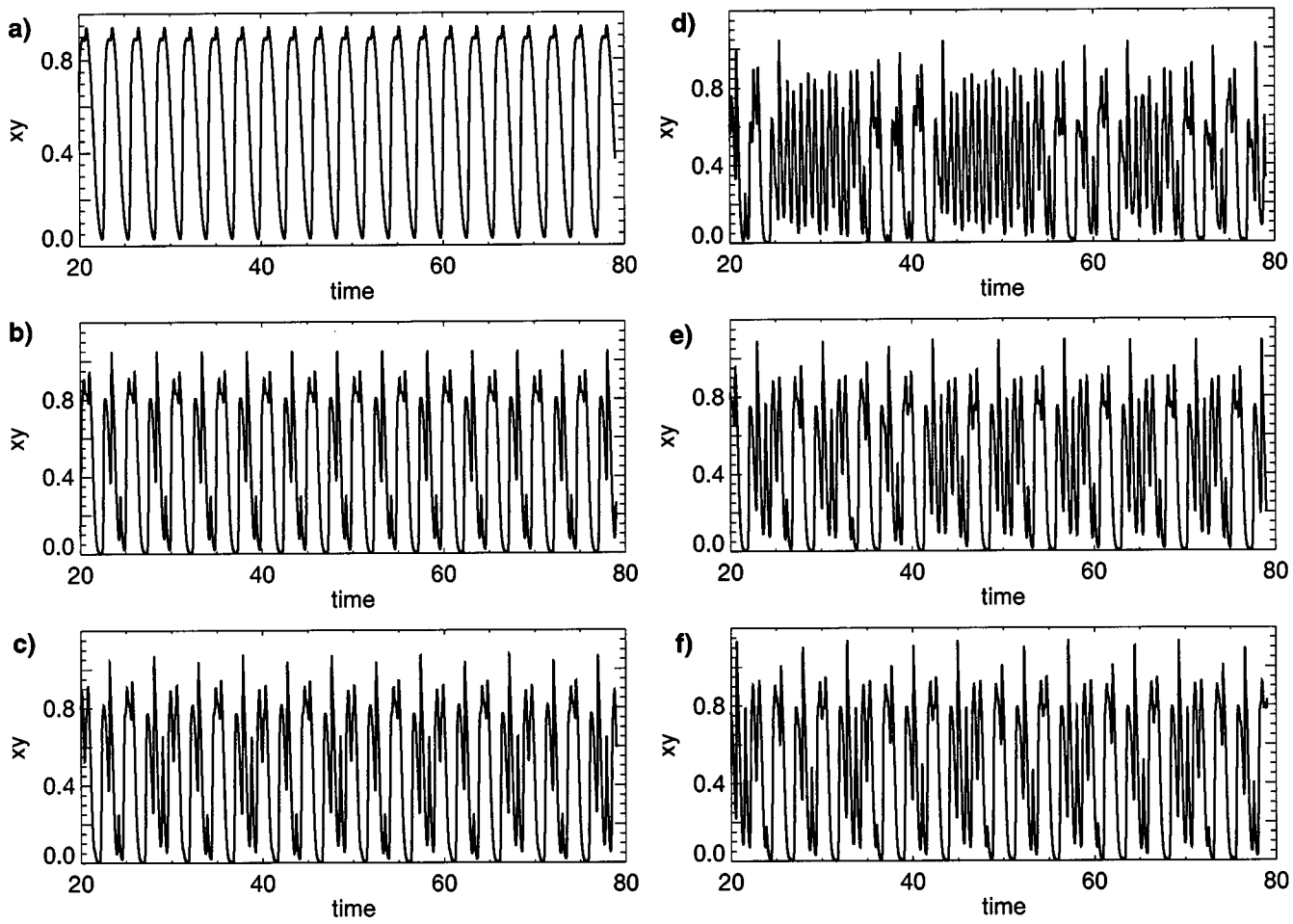


FIG. 4. Oscillations in the dimensionless reaction rate $xy$ obtained by numerical integration of Eqs. (8) and (9) with $G=16$, $\nu=9$; (a) period-1 oscillations, $a=340$, $g=4$; (b) period-2 oscillations, $a=200$, $g=7.5$; (c) period-4 oscillations, $a=164.5$, $g=8$; (d) chaotic oscillations, $a=90$, $g=10$, (e) a window of period-3, $a=150$, $g=8.5$; (f) a window of period-5, $a=190$, $g=190$. Time is measured in units of the delay time $\tau$.

where the last term corresponds to heterogeneous nucleation at static defects whose intensity is characterized by the coefficient $B$, proportional to the total number $n_0$ of static defects on the surface.

After adiabatic elimination of the coverage $c$ and a transition to dimensionless variables $x$ and $y$, defined above, the earlier system of Eqs. (8) and (9) is replaced by

$$G^{-1}\dot{x}+x=1-xy, \tag{14}$$

$$g^{-1}\dot{y}+y=a[x(t-1)]^{\nu+1}y(t-1)+b[x(t-1)]^{\nu}, \tag{15}$$

where the coefficients are $a=A\alpha^{\nu}p_0^{\nu+1}/\mu\gamma^{\nu}$ and $b=Bk\alpha^{\nu}p_0^{\nu}/\Gamma\mu\gamma^{\nu}$. Note that the parameter $b$ specifies now the relative intensity of the heterogeneous nucleation at static defects.

Figure 5 presents the bifurcation diagram in the plane $(a,b)$ obtained by numerical integrations of Eqs. (14) and (15). We see that for small values of the coefficient $b$ the behavior of the system is not significantly changed. However, when the contribution of heterogeneous nucleation at static defects increases (i.e., for larger values of the coefficient $b$),the chaotic region narrows and finally disappears. At large values of $b$, only simple period-1 oscillations are found in the system.

Thus, we conclude that heterogeneous nucleation of new islands at defects generated by the reaction is an essential element of the model. When this process is absent or dominated by heterogeneous nucleation at permanent structural defects, chaotic oscillations of the reaction rate cannot develop.

## V. MODIFICATIONS OF THE BASIC MODEL

The basic model given by Eqs. (1)–(3) and (6) is aimed only at the identification of the mechanism which is responsible for the onset of chaotic oscillations in surface reactions. Hence, it neglects many actual aspects of the reactions (and includes, for instance, only one reacting species). Obviously, one should therefore not expect that this model yields quantitatively correct predictions which could be directly compared with the experimental data.

Nonetheless, there are two properties of the model which might be seen as its potential deficiencies. First, as shown in Fig. 4, the reaction rate, $r$, oscillates with a large amplitude

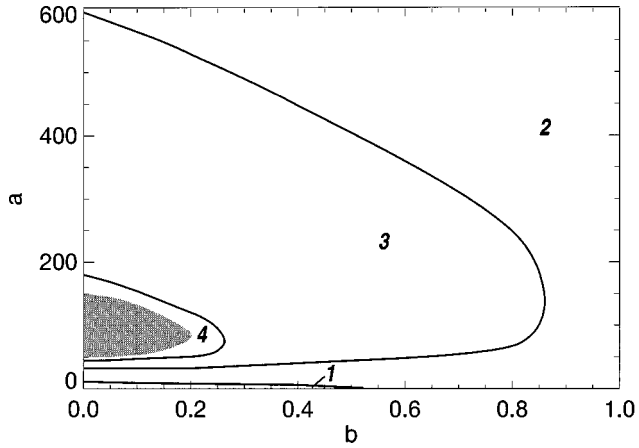


FIG. 5. Bifurcation diagram in the plane $(a,b)$ for the dynamical systems (14) and (15) for $G=16$, $\nu=9$, $g=8$; (1) damped oscillations resulting in a stable steady state, (2) period-1 oscillations, (3) period-2 oscillations, (4) period-4 oscillations. The gray region indicates long period oscillations and chaotic regimes.

and reaches very small values at its minimum. In contrast to this, in the experiments[5] the rate oscillations are always found superimposed on a substantial steady level. Second, it turns out that kinetic rate oscillations are accompanied by large variations of the partial pressure $p$ of the reagent in the gas phase, while in the experiments these pressure variations do not actually exceed 10%.

Below we show that both deficiencies can be corrected by small modifications of the basic model.

First, it is natural to assume that, besides the temporary reactive area provided by the growing and dying islands, the surface also includes some permanently reactive regions. Such regions may, for instance, develop near strong structural defects of the surface. If the total area occupied by these permanently reactive islands is $q_{\mathrm{def}}$, we must replace $q$ in Eq. (3) by the sum of $q+q_{\mathrm{def}}$. In Eq. (10) for the dimensionless partial pressure $x=p/p_0$ the term $xy$ is then replaced by the term $x(y+y_0)$ where $y_0=kq_{\mathrm{def}}/\Gamma$. Hence, we have now the dynamical system,

$$G^{-1}\dot{x}+x=1-x(y+y_0), \tag{16}$$

$$g^{-1}\dot{y}+y=a[x(t-1)]^{\nu+1}y(t-1). \tag{17}$$

Numerical simulations of this modified model have shown that it has qualitatively the same bifurcation diagram as the original system of Eqs. (9) and (10). The only difference is that the entire diagram is shifted to higher levels of the parameter $a$, i.e., higher nucleation rates are now needed to produce oscillations. However, the profile of oscillations undergoes an important change. As shown in Fig. 6, oscillations of the dimensionless reaction rate $r=x(y+y_0)$ remain now well above zero for all typical oscillation regimes.

The right column in Fig. 6 shows the corresponding oscillations in the partial pressure $x=p/p_0$ in the model given by Eqs. (16) and (17). We see that their magnitude is still too large, but this can be eliminated by another modification of the model. As an approximation for the coverage dependence of the island nucleation rate, a simple power-law dependence $f(c)=f_0c^{\nu}$ has been chosen above. It can, however, be expected that island nucleation is possible only after a certain critical coverage $c_{\mathrm{cr}}$ is exceeded, i.e., that the function $f(c)$ is zero for $c<c_{\mathrm{cr}}$.

Indeed, according to the statistical theory of first-order phase transitions in condensed systems,[32] regions of a new phase can nucleate only when they correspond to a thermodynamically favorable state. Thus, nucleation occurs only after the line of stationary coexistence of two phases is crossed. Similar behavior holds when heterogeneous nucleation on defects that facilitate formation of a nucleus is considered. In terms of the adsorbate coverage outside of the islands, the line of stationary coexistence of two phases may correspond to a certain critical coverage $c_{\mathrm{cr}}$. The size of a critical nucleus goes to infinity there[32] which means that the nucleation becomes increasingly less probable as this line is approached, i.e., the nucleation rate reaches zero at $c=c_{\mathrm{cr}}$.

A complete theory of island nucleation in the considered systems is still absent and the above general arguments are not intended to replace it. However, if we follow them, a possible phenomenological choice of the dependence $f(c)$ can be

$$f(c)=\begin{cases}0, & \text{for} \quad c<c_{\mathrm{cr}}\\ f_0(c-c_{\mathrm{cr}})^{\nu}, & \text{for} \quad c\geqslant c_{\mathrm{cr}}.\end{cases} \tag{18}$$

When this dependence, together with the existence of a permanently reactive surface area, is incorporated into our basic model, it yields, after adiabatic elimination of the coverage $c$ and a transition to dimensionless variables, the following system of two differential delay equations:

$$G^{-1}\dot{x}+x=1-x(y+y_0), \tag{19}$$

$$g^{-1}\dot{y}+y=\begin{cases}0, & \text{for} \quad x(t-1)<x_{\mathrm{cr}}\\ \alpha[x(t-1)-x_{\mathrm{cr}}]^{\nu}y(t-1)x(t-1), & \text{for} \quad x(t-1)>x_{\mathrm{cr}},\end{cases} \tag{20}$$

where the coefficients are $G=\Gamma\tau$, $g=\mu\tau$, $a=A\alpha^{\nu}p_0^{\nu+1}/\mu\gamma^{\nu}$, $y_0=kq_{\mathrm{def}}/\Gamma$, and $x_{\mathrm{cr}}=\gamma c_{\mathrm{cr}}/\alpha p_0$.

Figure 7 shows the bifurcation diagram in the plane $(a,\nu)$ obtained by numerical integration of the modified Eqs. (19) and (20) for $x_{\mathrm{cr}}=0.6$ and $y_0=0.2$. The main difference to the original bifurcation diagram (Fig. 2) of the initial model is that the region with chaotic oscillations extends now to smaller values of the exponent $\nu$, i.e., chaotic oscil-

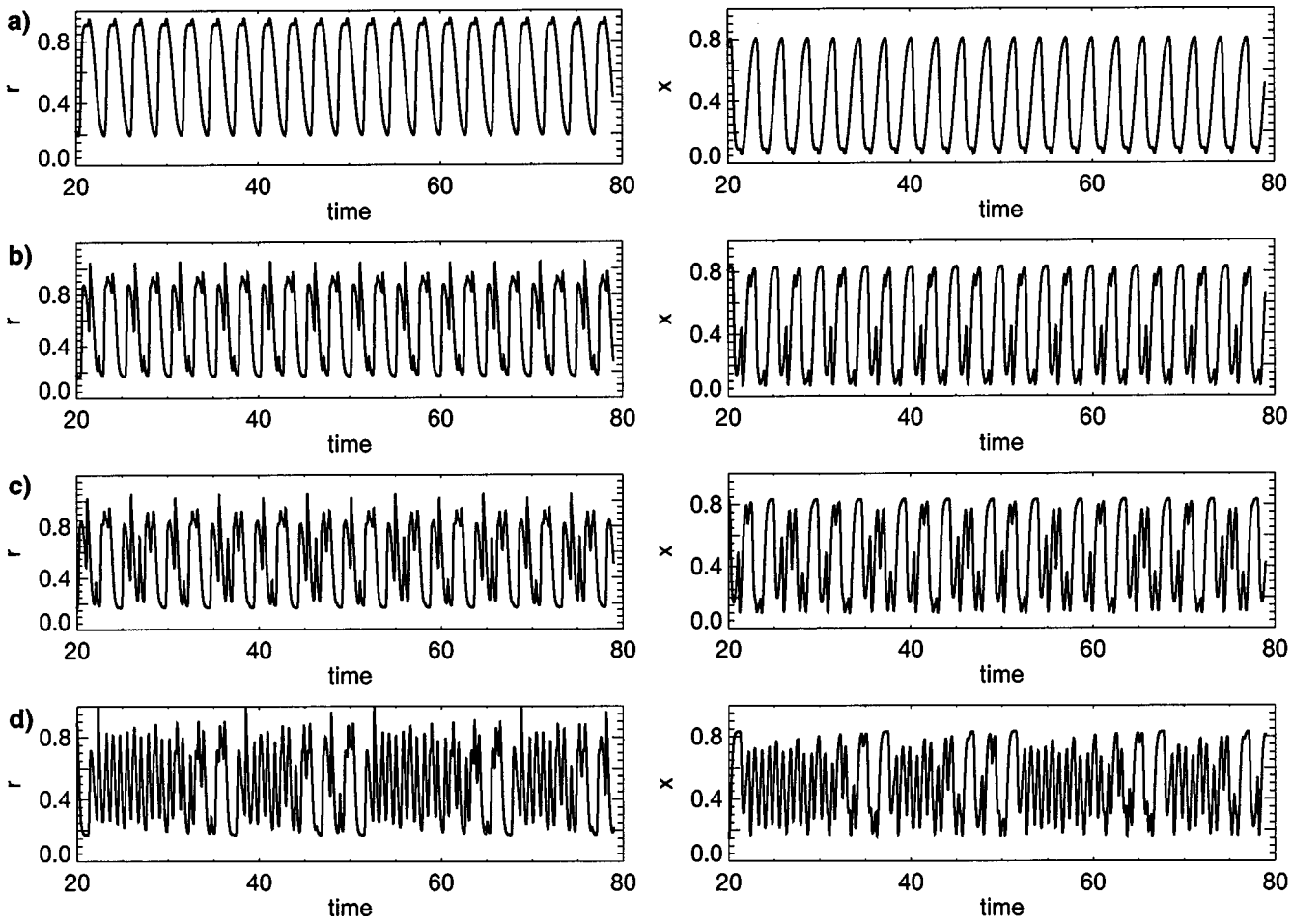


FIG. 6. Oscillations in the dimensionless reaction rate $r=x(y+y_0)$ (left) and in the dimensionless partial pressure $x=p/p_0$ (right) obtained by numerical integration of Eqs. (16) and (17) with $G=16$, $\nu=9$, $y_0=0.2$; (a) period-1 oscillations, $a=2000$, $g=4$; (b) period-2 oscillations, $a=1500$, $g=7.5$; (c) period-4 oscillations, $a=1000$, $g=8$; (d) chaotic oscillations, $a=550$, $g=9$. Time is measured in units of the delay time $\tau$.

lations can be found already at $\nu=4$ instead of 7 as in the earlier model. Note that in order to reach the same characteristic nucleation rates, much larger values of the coefficient $a$ in the equation for $y$ now have to be chosen.

The bifurcation diagram for Eqs. (19) and (20) in the plane $(a,g)$ which is shown for $\nu=6$ in Fig. 8 is similar to the respective diagram obtained for the original model (Fig. 3). Therefore, the same sequence of instabilities under increasing temperature is found in the modified model.

Oscillations in the reaction rate $r$ and in the partial pressure of the reactant for different regions in the bifurcation diagram of the modified model are shown in Fig. 9. Similar to Eqs. (16) and (17), the reaction rate remains well above zero. The most important effect, however, is that the magnitude of the partial pressure variations is now strongly reduced and lies in an interval from 7% to 10%, in reasonable agreement with the experimental data.

## VI. DISCUSSION

Chaotic behavior of reaction rates in catalytic reactions can in principle originate from (i) the chaotic dynamics of local oscillators, (ii) the development of irregular spatiotemporal modes, (iii) nonuniformities of the catalyst in connection with diffusional, thermal or gas-phase coupling, and (iv) synchronization and delayed response due to global coupling. Spatiotemporal chaos can develop in a pattern forming system, for example, through a spiral breakup mechanism[33] but for large extended systems some kind of coherence or synchronization would still be required in order to produce macroscopic variations in the reaction rate.[34] Accordingly, though spatiotemporal chaos has found widespread theoretical interest, the connection to experimentally observed chaotic oscillations in the reaction rate has so far not been established.

Naturally, since even very well prepared single crystal surfaces are never perfectly uniform but exhibit a large number of microscopic and also some macroscopic defects, the idea of nonuniformities being responsible for chaotic behavior has been pursued in several theoretical investigations. In high pressure experiments with supported catalysts the material is clearly highly nonuniform.[1] The behavior of such a catalyst was simulated by Schüth *et al.* who showed that chaotic rate oscillations can easily be generated in an ensemble of thermally coupled oscillators by introducing

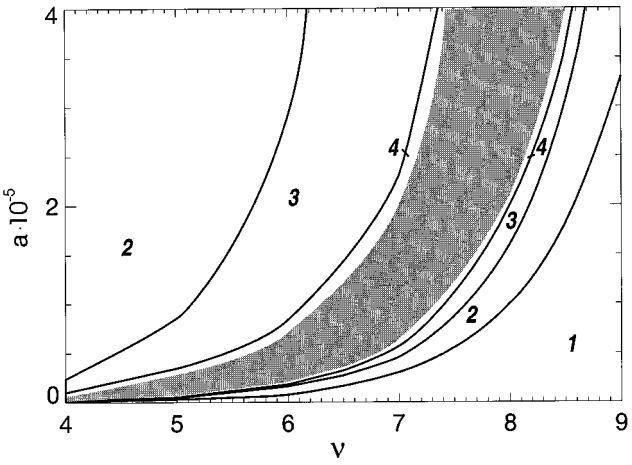


FIG. 7. Bifurcation diagram in the plane $(a,\nu)$ for the dynamical systems (19) and (20) for $G=50$, $g=8$, $\nu=6$, $y_0=0.2$, $x_{cr}=0.6$; (1) damped oscillations resulting in a stable steady state, (2) period-1 oscillations, (3) period-2 oscillations, (4) period-4 oscillations. The gray region indicates long period oscillations and chaotic regimes.

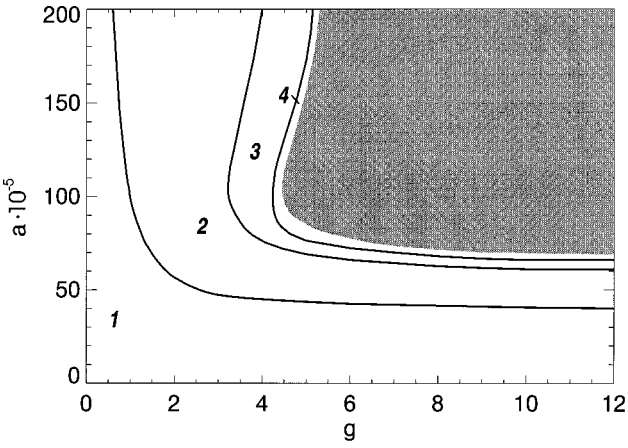


FIG. 8. Bifurcation diagram in the plane $(a,g)$ for the dynamical systems (19) and (20) for $G=50$, $\nu=6$, $y_0=0.1$, $x_{cr}=0.8$; (1) stable steady state, (2) period-1 oscillations, (3) period-2 oscillations, (4) period-4 oscillations. Complex oscillations and chaotic regimes are found inside the gray region.

nonuniformities.[35] In order to explain the chaotic rate oscillations which occur in catalytic CO oxidation on Pt(110) Savchenko suggested a model in which the amount of subsurface oxygen varies spatially.[36] This model, however, assumes that subsurface oxygen formation and not the $1\times1\leftrightarrow1\times2$ phase transition is the driving force for the oscillations which is in contradiction to most experimental studies.[2]

Spatial nonuniformities do of course also exist on Pt(100) but since experiments with two different Pt(100) single crystals yielded nearly the same Feigenbaum transition to chaos in the NO+CO reaction, the nonuniformities of the surface can hardly be decisive for the development of chaos.[5,25] Moreover, since two different chemical reactions, NO+CO and NO+ $H_2$, exhibit very similar chaotic behavior on Pt(100) with both reactions undergoing a Feigenbaum transition to chaos, the details of the chemistry are apparently of no strong importance for the chaotic behavior.[4,5] Since the region in parameter space in which the chaotic oscillations are observed coincides with the region in which the different local oscillators have to synchronize in order to generate macroscopic rate oscillations, an explanation based on synchronization appears to be compelling (see Fig. 1). The simulation results presented in the paper (though the model is strongly simplified) essentially confirm this idea.

It is close-lying to see whether the same model for chaos can also be applied to the system Pt(110)/CO+$O_2$. Similar to the present system a surface phase transition, namely $1\times1\leftrightarrow1\times2$, is involved and a Feigenbaum scenario to chaos is observed in the transition of the reaction rate from oscillatory to stationary behavior.[3] This indicates that also in this system the appearance of chaos is connected with the breakdown of global coupling. At present a participation of the spatial degrees of freedom in the chaotic regime cannot definitely be excluded but it appears rather likely that the model presented here can with some modifications also be applied to Pt(110)/CO + $O_2$.

The model introduced in this paper is a skeleton model which neglects many details of adsorption, reaction, and diffusion and of the phase transition. Within this strongly simplified model a number of assumptions have been made whose justification needs to be discussed in more detail.

An essential point of the model is the existence of a critical radius beyond which the $1\times1$ adsorbate islands become unstable and dissolve. In order to find possible sources of instability for these islands one has to examine the situation of a growing $1\times1$ adsorbate island more closely. The islands grow through CO/NO molecules which are trapped at the edge of the island while the coverage far in the interior of the island is mainly determined by an adsorption/desorption equilibrium. If with growing island size the diffusion inside the island is no longer efficient enough to remove the resulting concentration gradient between the edge and the interior of the island, it might occur that the coverage in the interior of the island falls below the stability limit of 0.5 thereby igniting the ''surface explosion.'' A second factor leading to a critical size might be that with increasing size the island will have a high probability of getting in contact with structural defects which due to their enhanced efficiency in dissociating NO can ignite the ''surface explosion'' likewise.[7,24]

These considerations also show that it would be more realistic to calculate with a distribution of island sizes and to include stochastic elements instead of referring to a single critical island size as was done here. A second conclusion which can be drawn from the above discussion is that in addition to synchronization via nucleation the islands can also synchronize at the moment when they become reactive. Since the stability of the adsorbate islands is on a critical borderline, it is very plausible that small variations in the partial pressures of CO and NO and hence in the adsorbate coverages can exert a strong stabilizing or destabilizing ef-

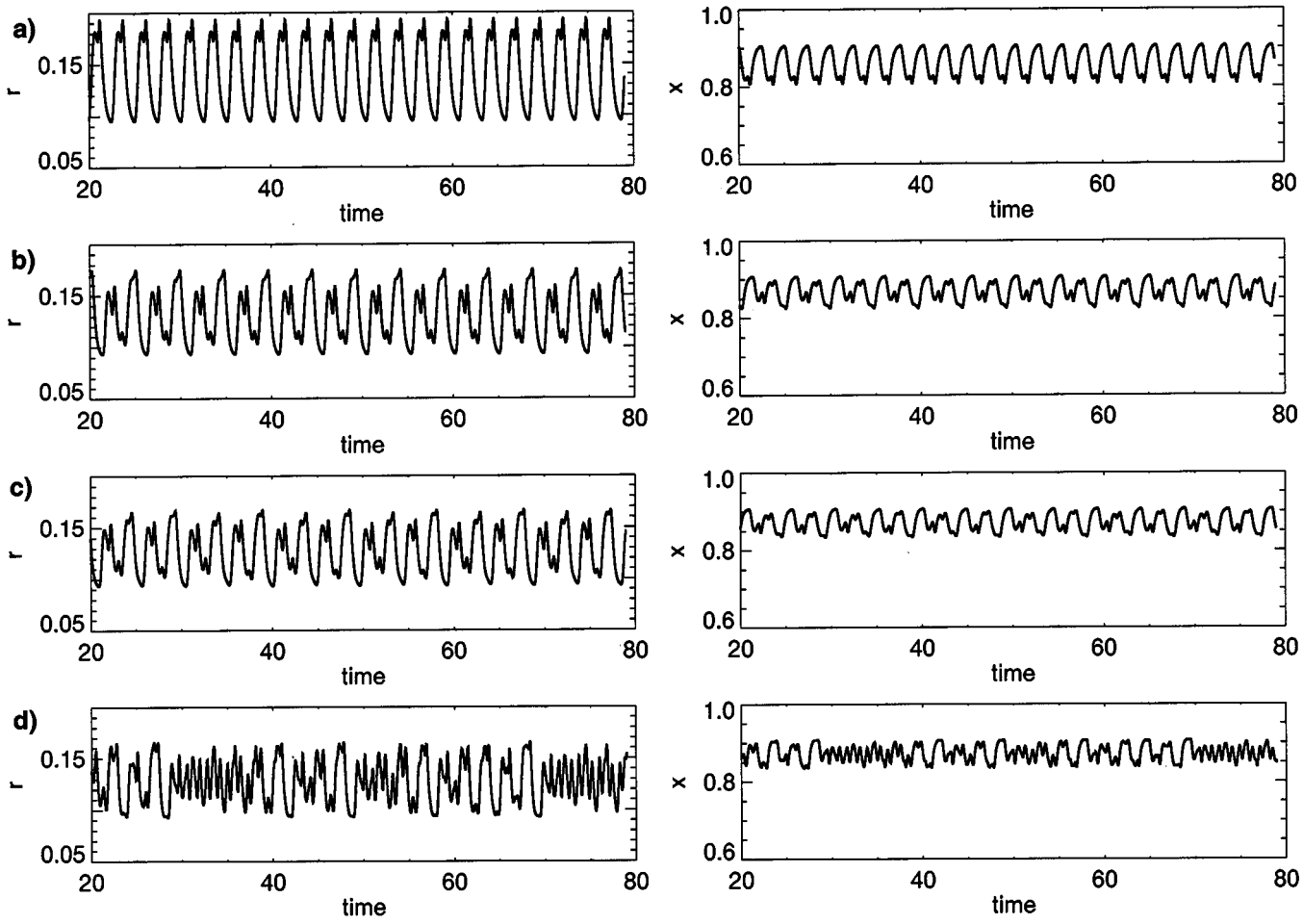


FIG. 9. Oscillations in the dimensionless reaction rate $r=x(y+y_0)$ (left) and in the dimensionless partial pressure $x=p/p_0$ (right) obtained by numerical integration of Eqs. (19) and (20) with $G=50$, $\nu=6$, $y_0=0.1$, $x_{cr}=0.8$; (a) period-1 oscillations, $a=1.5\times10^7$, $g=3$; (b) period-2 oscillations, $a=1\times10^7$, $g=4$; (c) period-4 oscillations, $a=0.88\times10^7$, $g=4.5$; (d) chaotic oscillations, $a=0.85\times10^7$, $g=7$. Time is measured in units of the delay time $\tau$.

fect, thus synchronizing the population of islands. One can introduce this additional synchronizing effect into the model by making the critical radius/lifetime of the islands pressure dependent. Some calculations which included this additional dependence have been conducted but the result was that, at least within the context of this skeleton model, this effect is of no decisive importance for the development of chaotic behavior.

Another possible direction of further research is to try to deduce directly from the experimental data whether delays are involved in the experimentally observed chaotic oscillations. In this respect, it should be noted that the statistical analysis of experimental time series which has so far been performed for such oscillations[3,4] does not allow us to distinguish between nonlinear and delay-induced chaotic oscillations. However, new more refined ways of data processing are being developed which can make this distinction possible, as has already been demonstrated for a simple example of a single-variable delay system.[37]

## VII. CONCLUSIONS

We have shown that deterministic chaos in catalytic surface reactions can have its origin in a failure of the synchronization process as the delay between global coupling and the response of the surface reaction begins to dominate the dynamics. A skeleton model was presented describing a surface reaction which on a macroscopic scale oscillates spatially uniformly but on a microscopic scale consists of isolated islands globally coupled together via the gas phase. The simulations reproduce qualitatively the Feigenbaum scenario and the chaotic rate oscillations studied experimentally with the systems Pt(100)/NO+CO and Pt(100)/NO + $H_2$. Synchronization in these systems takes place via the adsorbate-induced $1\times1\leftrightarrow$hex surface phase transition of Pt(100).

It has turned out that the precise formulation of the nucleation and growth kinetics is of decisive importance for reproducing the experimental observations. In order to further develop the model, more information, preferably by *in situ* experiments, is required about the nucleation and growth of the $1\times1$ islands under reaction conditions. Global synchronization via gas-phase coupling is a rather general phenomenon in surface reactions exhibiting oscillatory reaction rates and accordingly the model presented here should be applicable to a rather wide range of systems.

## ACKNOWLEDGMENTS

The authors thank D. A. King for elucidating some of his experimental results. Financial support of the Volkswagen-Stiftung is gratefully acknowledged.

[1] M. Eiswirth, in *Chaos in Chemistry and Biochemistry*, edited by R. J. Fields and L. Györgyi (World Scientific, Singapore, 1993).
[2] R. Imbihl and G. Ertl, Chem. Rev. **95**, 697 (1995).
[3] M. Eiswirth, K. Krischer, and G. Ertl, Surf. Sci. **202**, 565 (1988).
[4] P. D. Cobden, J. Siera, and B. E. Nieuwenhuys, J. Vac. Sci. Technol. A **10**, 2487 (1992).
[5] G. Veser, F. Mertens, A. S. Mikhailov, and R. Imbihl, Phys. Rev. Lett. **71**, 935 (1993); G. Veser and R. Imbihl, J. Chem. Phys. **100**, 8492 (1994).
[6] K. Krischer, M. Eiswirth, and G. Ertl, J. Chem. Phys. **96**, 9161 (1992).
[7] T. Fink, J.-P. Dath, R. Imbihl, and G. Ertl, J. Chem. Phys. **95**, 2109 (1991).
[8] A. Hopkinson and D. A. King, Chem. Phys. **177**, 433 (1993).
[9] S. J. Lombardo, T. Fink, and R. Imbihl, J. Chem. Phys. **98**, 5526 (1993).
[10] M. Gruyters, A. T. Pasteur, and D. A. King, J. Chem. Soc. Faraday Trans. **92**, 2941 (1996).
[11] N. Khrustova, G. Veser, A. Mikhailov, and R. Imbihl, Phys. Rev. Lett. **75**, 3564 (1995).
[12] R. J. Behm, P. A. Thiel, P. R. Norton, and G. Ertl, J. Chem. Phys. **78**, 7437, 7448 (1983).
[13] F. Ritter, R. J. Behm, G. Pötschke, and J. Wintterlin, Surf. Sci. **181**, 403 (1987); W. Hösler, E. Ritter, and R. J. Behm, Ber. Bunsenges. Phys. Chem. **90**, 205 (1986).
[14] A. Crossley and D. A. King, Surf. Sci. **95**, 131 (1990).
[15] K. Heinz, E. Lang, K. Strauss, and K. Müller, Appl. Surf. Sci. **11/12**, 611 (1982).
[16] A. Hopkinson, X.-C. Guo, J. M. Bradley, and D. A. King, J. Chem. Phys. **99**, 8262 (1993).
[17] A. Hopkinson, J. M. Bradley, X.-C. Guo, and D. A. King, Phys. Rev. Lett. **71**, 1597 (1993).
[18] A. Borg, A.-M. Hilmen, and E. Bergene, Surf. Sci. **306**, 10 (1994).
[19] P. Gardner, R. Martin, M. Tüshaus, and A. M. Bradshaw, J. Electron. Spectrosc. Relat. Phenom. **54/55**, 619 (1990).
[20] Y. Y. Yeo, C. E. Wartnaby, and D. A. King, Science **268**, 1731 (1995).
[21] A. T. Pasteur, St. J. Dixon-Warren, and D. A. King, J. Chem. Phys. **103**, 2251 (1995).
[22] T. Fink, J.-P. Dath, M. R. Bassett, R. Imbihl, and G. Ertl, Surf. Sci. **245**, 96 (1991).
[23] M. W. Lesley and L. D. Schmidt, Surf. Sci. **155**, 215 (1985).
[24] Y. Uchida, R. Imbihl, and G. Lehmpfuhl, Surf. Sci. **275**, 253 (1992).
[25] G. Kierspel (unpublished data).
[26] R. May, Nature **261**, 459 (1976).
[27] M. C. MacKey and L. Glass, Science **197**, 287 (1977).
[28] K. Ikeda, H. Daido, and O. Akimoto, Phys. Rev. Lett. **45**, 709 (1980).
[29] P. Nardone, P. Mandel, and R. Kapral, Phys. Rev. A **33**, 2465 (1986).
[30] D. A. King (private communication).
[31] A. S. Mikhailov and A. Yu. Loskutov, *Foundations of Synergetics II. Chaos and Noise*, 2nd revised edition (Springer, Berlin, 1996).
[32] L. D. Landau and E. M. Lifshitz, *Statistical Physics* (Pergamon, Oxford, 1980).
[33] M. Bär and M. Eiswirth, Phys. Rev. E **48**, R1635 (1993).
[34] H. Levine and X. Zou, Phys. Rev. Lett. **66**, 204 (1992); F. Mertens, R. Imbihl, and A. Mikhailov, J. Chem. Phys. **99**, 8668 (1993); **101**, 9903 (1994); M. Falcke and H. Engel, *ibid*. **101**, 6255 (1994).
[35] F. Schüth, X. Song, L. D. Schmidt, and E. Wicke, J. Chem. Phys. **92**, 745 (1990).
[36] V. I. Savchenko, Mendeleev Commun. **1991**, 139.
[37] M. J. Bünner, M. Popp, T. Meyer, A. Kittel, and J. Parisi, in *Nonlinear Physics of Complex Systems*, edited by J. Parisi, S. Müller, and W. Zimmermann (Springer, Berlin, 1996), pp. 229–238.